sciendo

LATVIAN JOURNAL OF PHYSICS
AND TECHNICAL SCIENCES
2018, N 5

DOI: 10.2478/lpts-2018-0034

SOLID STATE PHYSICS

FIRST-PRINCIPLES MODELLING OF N-DOPED Co_3O_4

G.A. Kaptagay[1], Yu.A. Mastrikov[2], E.A. Kotomin[2]

[1] Kazakh State Women's Teacher Training University, Almaty, Kazakhstan
[2] Institute of Solid State Physics, University of Latvia

N-doped Co_3O_4 is a promising electrocatalyst. By means of first-principles calculations, various concentrations and spatial arrangements of N_O atoms were modelled. Mutual interaction of the dopant atoms was analysed with respect to single N_O atom. Charge redistribution, caused by doping, was calculated.

Keywords: Co_3O_4, OER, electrocatalyst

1. INTRODUCTION

Oxygen Evolution Reaction (OER) is the essential process for many rapidly developing applications, such as energy conversion and storage [1]. Water splitting devices, some types of fuel cells as well as rechargeable batteries require an effective OER electrocatalyst. Performance of the catalyst depends on overpotential. Noble metal oxides RuO_2 and IrO_2 with low overpotential demonstrate high performance [2]. The cost of these materials, however, limits their usage. Relatively low overpotential of Co_3O_4 makes it a low-cost alternative of noble metal-based catalysts for OER [3], [4].

Numerous works show that overpotential of oxide catalyst can be reduced by doping [5]–[7]. Our earlier investigation confirms that doping Co_3O_4 by fluorine reduces overpotential, resulting in enhancement of catalytic activity [8]. Recent experimental study [9] demonstrates that doping Co_3O_4 by nitrogen, in the combination with oxygen vacancies, reduces overpotential, improving the overall electrocatalytic activity for OER.

Modelling of the surface reactions requires a preliminary study on the N-doped Co_3O_4 bulk. Analysing interaction energies of N atoms in Co_3O_4, we predict the most favourable spatial arrangement patterns for the dopant. Calculated electron charge redistribution reveals in detail the interaction between nitrogen atoms and Co_3O_4.

2. METHOD AND MODEL

Calculations were performed using the DFT method [10], as implemented in the computer code VASP 5.4 [11]. Applicability of the method to the system under study was already tested [8]. Core electrons were substituted by the US potentials with the PAW method [12] applied.

Table 1

US PAW Potentials of Co and O

Element	Free electrons	E_{cutoff}, eV
Co	$4s^1 3d^8$	267.968
O	$2s^2 2p^4$	400.000
N	$2s^2 2p^3$	400.000

Exchange-correlation was described by the PBE functional [13]. The Hubbard correction U-J=3eV [14] was applied to d-electrons of Co_{tet} as well as Co_{oct} atoms. Spin polarization was implemented in the AAF order, alternating on the Co_{tet} planes. For defects modelling cubic 56-atom supercell model was used. Brillouine zone [15] was sampled with the 2x2x2 Monkhorst-Pack [16] scheme. Plain-waive basis set has the kinetic energy cut-off of 550eV. Charge redistribution was analysed by the Bader method [17], as implemented by Henkelmann et al. [18], [19].

Co_3O_4 has a structure of normal spinel, symmetry group 227 [20]. The tetragonal 8*a* sites are occupied by Co^{2+}, and the octahedral 16*d* sites by Co^{3+}. O^{2-} ions occupy 32*e* sites.

Doping by nitrogen was performed by substitution of oxygen atoms. Four concentrations were tested – 1, 2, 4 and 8 N per 32(O+N) atoms. There are five non-equivalent distances between 32 *e* sites in the supercell – 1–4 and 6NN (32*e*-32*e*). Some coordination spheres are split to the sub-spheres with a small deviation in distances as shown in Fig. 1.

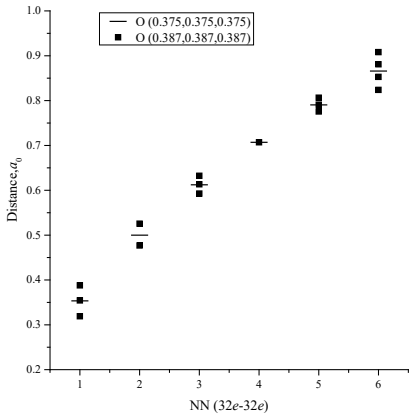

Fig. 1. Nearest neighbours of 32*e*-32*e* sites of Co_3O_4 structure, symmetry group 227.

Two N atoms were placed at each sub-sphere of the 1NN coordination sphere. For the 2NN single calculation was performed at the distance of the first sub-sphere. Two N atoms were also placed at the largest possible distance within the model supercell – 6NN, first subsphere. Four N atoms were arranged in three different configurations, as shown in Table 2.

Table 2

12.5% N Concentration Configurations. Distances between N_O in NN (32*e*-32*e*)

Conf.1	N_O	N_O	N_O	N_O
N_O	0	6	4	2
N_O		0	2	4
N_O			0	6
N_O				0

Conf.2	N_O	N_O	N_O	N_O
N_O	0	1	4	1
N_O		0	1	4
N_O			0	1
N_O				0

Conf.3	N_O	N_O	N_O	N_O
N_O	0	4	4	4
N_O		0	4	4
N_O			0	4
N_O				0

Nanorod was created, by placing N atoms in line, along the [110]. All N atoms in the same line are the 1NN. The smallest distance between the parallel rods is 3NN (Table 3).

Table 3

25% N Concentration Configurations. Distances between N_O in NN (32*e*-32*e*)

	N_O	N_O	N_O	N_O	N_O	N_O	N_O	N_O
N_O	0	1	4	1	4	3	3	4
N_O		0	1	4	3	4	4	3
N_O			0	1	4	3	3	4
N_O				0	3	4	4	3
N_O					0	1	1	4
N_O						0	4	1
N_O							0	1
N_O								0

3. RESULTS

Two N_O atoms, placed at various distances, exhibited predominantly repulsive interaction, except for the smallest possible distance (-0.02eV). The absolute energy values, however, do not exceed 0.1 eV, which characterises the N_O-N_O interaction in Co_3O_4 as neutral (Fig. 2).

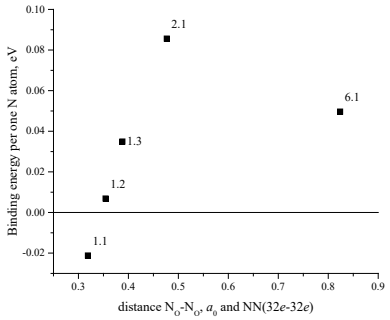

Fig. 2. Binding energy between two N_O doping atoms in Co_3O_4, per N_O atom, depending on the distance.

The N_O-N_O interaction at higher concentrations strongly depends on a particular configuration of the doping atoms (Fig. 3). The lowest energy of -0.03eV corresponds (Conf. 2, Table 2) to a high number of the N_O-N_O 1NN. The most uniform distribution of N_O (Conf. 3 Table 2) gives intermediate repulsion energy of 0.09 eV. The highest binding energy of three calculated configurations of 0.125% is 0.12eV, which can be explained by the presence of the N_O-N_O 2NN bonds (Conf. 1 Table 2) with relatively strong repulsion (Fig. 1).

Aligned in line (Table 3), N_O atoms create stable nano-chains with the binding energy of 0.02eV per atom. Obviously, in such a configuration the primary interaction occurs between the 1NN.

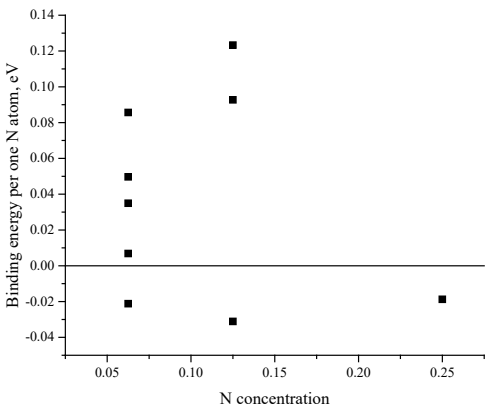

Fig. 3. Binding energy between N_O doping atoms in Co_3O_4, per N_O atom.

Electron charge redistribution, in comparison with undoped Co_3O_4, is localised on the nearest to the dopant Co cations. With respect to oxygen anion, nitrogen anion in Co_3O_4 is less negative. Therefore, Co cations become less positive. Configurations with the lowest binding energy values demonstrate relatively high charge transfer (-0.05 *e*) from the N_O-N_O 1NN pairs to the nearest Co_{tet} - Table 4 (N 1.1NN, Table 2 Conf.2, Table 3 Conf.). For the configuration with the strongest repulsion between N_O-N_O (N 2.1NN), the largest charge value -0.07 *e* was observed on Co_{oct}.

Table 4

Electron Charge Redistribution on Co_{tet} and Co_{oct} Cations in *e*, with respect to the Pure Co_3O_4. Multiplicity of Co cations is given per N_O atom.

single N		
mult.	N	0.02
1	Co_{tet}	-0.02
3	Co_{oct}	-0.02

N 1.1NN		
mult.	N	0.03
1	Co_{oct}	-0.05
1	Co_{oct}	-0.02

N 1.2NN		
mult.	N	0.03
1	Co_{tet}	-0.02
1	Co_{oct}	-0.02
1	Co_{oct}	-0.02
0.5	Co_{oct}	-0.03

N 1.3NN		
mult.	N	0.02
2	Co_{oct}	-0.02
1	Co_{oct}	-0.02

N 2.1NN		
mult	N	0.03
2	Co_{oct}	-0.02
0.5	Co_{oct}	-0.07

N 6.1NN		
mult.	N	0.02
1	Co_{tet}	-0.02
3	Co_{oct}	-0.02

Table 2, Conf.1		
mult.	N	0.03
0	Co_{tet}	
2	Co_{oct}	-0.03
0.5	Co_{oct}	-0.05

Table 2, Conf.2		
mult.	N	0.02
0.5	Co_{tet}	-0.06
1	Co_{oct}	-0.01
1	Co_{oct}	-0.03

Table 2, Conf.3		
mult	N	0.03
1	Co_{tet}	-0.03
3	Co_{oct}	-0.03

Table 3. Conf.		
mult.	N	0.03
0.5	Co_{tet}	-0.06
1	Co_{oct}	-0.04
1	Co_{oct}	-0.02

4. CONCLUSIONS

Small differences (<0.15eV) in interaction energies between various spatial arrangements indicate that in Co_3O_4 oxygen is easily substituted by nitrogen and at room temperature N atoms can be distributed in the material randomly. Repulsive interaction (<0.13eV) between the dopant atoms has been observed for most concentrations and configurations of N_O in Co_3O_4, except for the 1NN. All structures with dominating 1NN interaction, consistently exhibited energetic stability (-0.02-0.03eV), in contrast to other configurations. Binding between two nearest N_O cations is facilitated by an intense electron charge exchange (0.05*e*) with the nearest to both dopant atoms Co_{tet}. Depending on a particular configuration, high charge transfer (>0.05*e*) may show both Co_{tet} and Co_{oct} atoms. The performed calculations create a solid base for the further modelling of OER on N-doped Co_3O_4 surface.

ACKNOWLEDGEMENTS

The project Nr. AP05131211 "First Principles Investigation on Catalytic Properties of N-doped Co_3O_4" is supported by the Ministry of Education and Science of the Republic of Kazakhstan within the framework of the grant funding for scientific and (or) scientific and technical research for 2018-2020. The authors thank T. Inerbaev and A. Popov for fruitful discussions and valuable suggestions. Yu.M. thanks M.Putnina for the technical assistance in preparation of the manuscript.

REFERENCES

1. Cook, T., Dogutan, D., Reece, S., Surendranath, Y., Teets, T., & Nocera, D. (2010). Solar energy supply and storage for the legacy and nonlegacy worlds. *Chemical Reviews, 110*(11), 6474–6502.
2. Reier, T., Oezaslan, M., & Strasser, P. (2012). Electrocatalytic oxygen evolution reaction (OER) on Ru, Ir, and Pt catalysts: A comparative study of nanoparticles and bulk materials. *ACS Catalysis, 2*(8), 1765–1772.
3. Zasada, F., Piskorz, W., Cristol, S., Paul, J.-F., Kotarba, A., & Sojka, Z. (2010). Periodic density functional theory and atomistic thermodynamic studies of cobalt spinel nanocrystals in wet environment: Molecular interpretation of water adsorption equilibria. *The Journal of Physical Chemistry C, 114*(50), 22245–22253.
4. Chen, J., & Selloni, A. (2012). Water adsorption and oxidation at the Co_3O_4 (110) surface. *The Journal of Physical Chemistry Letters, 3*(19), 2808–2814.
5. Liao, P., Keith, J., & Carter, E. (2012). Water oxidation on pure and doped hematite (0001) surfaces: Prediction of Co and Ni as effective dopants for electrocatalysis. *Journal of the American Chemical Society, 134*(32), 13296–13309.
6. Ohnishi, C., Asano, K., Iwamoto, S., Chikama, K., & Inoue, M. (2007). Alkali-doped Co_3O_4 catalysts for direct decomposition of N_2O in the presence of oxygen. *Catalysis Today, 120*(2), 145–150.
7. García-Mota, M., Vojvodic, A., Metiu, H., Man, I., Su, H.-Y., Rossmeisl, J., & Nørskov, J. (2011). Tailoring the activity for oxygen evolution electrocatalysis on rutile TiO_2(110) by transition-metal substitution. *ChemCatChem, 3*(10), 1607–1611.
8. Kaptagay, G., Inerbaev, T., Mastrikov, Y., Kotomin, E., & Akilbekov, A. (2015). Water interaction with perfect and fluorine-doped Co_3O_4 (100) surface. *Solid State Ionics, 277*, 77–82.
9. Xu, L., Wang, Z., Wang, J., Xiao, Z., Huang, X., Liu, Z., & Wang, S. (2017). N-doped nanoporous Co_3O_4 nanosheets with oxygen vacancies as oxygen evolving electrocatalysts. *Nanotechnology, 28*(16), 165402.
10. Kohn, W., & Sham, L. (1965). Self-consistent equations including exchange and correlation effects. *Physical Review, 140*(4A), A1133–A1138.
11. Kresse, G., & Furthmüller, J. (1996). Efficient iterative schemes for *ab initio* total-energy calculations using a plane-wave basis set. *Physical Review B, 54*(16), 11169–11186.
12. Blöchl, P. (1994). Projector augmented-wave method. *Physical Review B, 50*(24), 17953–17979.
13. Perdew, J., Burke, K., & Ernzerhof, M. (1996). Generalized gradient approximation made simple. *Physical Review Letters, 77*(18), 3865–3868.

14. Dudarev, S., Botton, G., Savrasov, S., Humphreys, C., & Sutton, A. (1998). Electron-energy-loss spectra and the structural stability of nickel oxide: An LSDA+U study. *Physical Review B, 57*(3), 1505–1509.
15. Brillouin, L. (1930). Les électrons libres dans les métaux et le role des réflexions de Bragg. *Journal de Physique et le Radium, 1*(11), 377–400.
16. Monkhorst, H., & Pack, J. (1976). Special points for Brillouin-zone integrations. *Physical Review B, 13*(12), 5188–5192.
17. R. F. Bader, R. F. (1990). *Atoms in Molecules: A Quantum Theory*. Oxford University Press, Oxford.
18. Henkelman, G., Arnaldsson, A., & Jónsson, H. (2006). A fast and robust algorithm for Bader decomposition of charge density. *Computational Materials Science, 36*(3), 354–360.
19. Yu, M., & Trinkle, D. (2011). Accurate and efficient algorithm for Bader charge integration. *The Journal of Chemical Physics, 134*(6), 064111.
20. Villars Pierre and Cenzual, K. (Ed.). (n.d.). Co_3O_4 Crystal Structure: Datasheet from "PAULING FILE Multinaries Edition – 2012"' in SpringerMaterials Available at https://materials.springer.com/isp/crystallographic/docs/sd_0311005
21. Springer-Verlag Berlin Heidelberg & Material Phases Data System (MPDS). Switzerland & National Institute for Materials Science (NIMS), Japan.

N-LEĢĒTĀ Co_3O_4 MODELĒŠANA PĒC PIRMAJIEM PRINCIPIEM

G. Kaptagaja, J. Mastrikovs, J. Kotomins

K o p s a v i l k u m s

N-leģētais Co_3O_4 ir perspektīvs elektrokatalizators. Izmantojot pirmā principa aprēķinus, tika modelētas dažādas N_O atomu koncentrācijas un telpiskās struktūras. Piemaisījuma atomu savstarpējā mijiedarbība tika analizēta attiecībā uz mono N_O atomu. Aprēķināts piemaisījumu radītais lādiņa pārdalījums.

30.08.2018.

Institute of Solid State Physics, University of Latvia as the Center of Excellence has received funding from the European Union's Horizon 2020 Framework Programme H2020-WIDESPREAD-01-2016-2017-TeamingPhase2 under grant agreement No. 739508, project CAMART²